

## On the Existence of $\alpha$ -Agostic Bonds: Bonding Analyses of Titanium Alkyl Complexes

Isaac Vidal,<sup>†</sup> Santiago Melchor,<sup>†</sup> Ibón Alkorta,<sup>‡</sup> José Elguero,<sup>‡</sup> Markku R. Sundberg,<sup>§</sup> and José A. Dobado<sup>\*,†</sup>

*Grupo de Modelización y Diseño Molecular, Departamento de Química Orgánica, Universidad de Granada, Av. Fuentenueva, s/n E-18071 Granada, Spain, Instituto de Química Médica CSIC, c/ Juan de la Cierva 3, E-28006 Madrid, Spain, and Laboratory of Inorganic Chemistry, Department of Chemistry, University of Helsinki, P.O. Box-55 (A.I. Virtasen Aukio 1) FIN-00014, Helsinki, Finland*

Received September 7, 2006

The main characteristics of the so-called “agostic bonding” in titanium complexes were computationally investigated in terms of diverse analyses, including the quantum theory of atoms in molecules (QTAIM) and the electron localization function (ELF). Computations on a set of titanium-based molecular models that were presumably able to present  $\alpha$ - and  $\beta$ -like bonding showed a clear distinction between  $\alpha$ - and  $\beta$ -bonding schemes. In view of the geometric, energetic, and electronic data of these molecules, we concluded that the geometries presenting a Ti $\cdots$ H approximation similar to  $\alpha$  bonding are not the result of a bonding attraction. On the contrary, their origin arises from a short-range repulsion between the metal core and the lone pairs of the alkylidene group, the latter pivoting in its own plane around carbon and thereby allowing simultaneously a closer approach between the Ti and the C atoms and indirectly resulting in a short Ti $\cdots$ H distance. Additionally, we found that the electronic and geometric distortion of the C–H bond present in the agostic bonding are not univocally linked to this kind of bonding; instead, this originates in the close distance of the C–H bond and any metal center, independently of whether it is due to an agostic bond or not. Therefore, the lengthening of the C–H bond and the reduction of its electron density at the bond critical point should not be considered as indication of agostic bonding but as a side effect.

### Introduction

In chemistry, the term agostic<sup>1</sup> is normally linked to the words “bonding” or “interaction”, depending on how the approximation between a C–H bond and a transition-metal atom in some organometallic compounds is interpreted. This concept, describing how the metal atom retains the alkyl hydrogen in a nearby position, has been also progressively extended to more polar bonds, including the attraction of Si–H or N–H bonds. Even at the time when the term “agostic” was coined,<sup>2</sup> it was evidenced that this interaction required special attention, and although its nature has been previously explained in terms of van der Waals radii<sup>3</sup> or as three-center–two-electron bonds,<sup>4</sup> a satisfactory determination of the causes that bring about this interaction is still missing.

Compounds presenting agostic interactions are of high relevance in organic synthesis, as the proximity of the H atom to the metal is accompanied by the activation of the C–H bond,<sup>5</sup>

thus constituting intermediate compounds in dehydrogenation reactions,<sup>6,7</sup> polymerization processes,<sup>8</sup> and even in stereospecific reactions.<sup>9</sup> Although C–H bonds are generally considered inert,<sup>10</sup> under specific conditions these bonds can be attracted toward a metal atom,<sup>11</sup> and transition metals are also easily inserted into organic bonds in several alkene metathesis processes. Within transition metals, some are more likely to induce agostic interactions than others, such as those from the IV group, Ti, Zr, and Hf, and the VIII group, whereas the agostic interactions are much more frequent for the second-row metals, Ru, Rh, and Pd. In general, the literature abounds with experimental data for second-row transition metals, while theoretical investigation is more focused on the first row.

Although these kinds of compounds received their name in the 1980s,<sup>2</sup> even today discussion continues regarding which model can best predict and rationalize agostic interactions. In a recent review,<sup>12</sup> the bonding model is revisited, pointing out that the conditions believed to cause the interaction<sup>2</sup> are not predictive enough to explain the absence of agostic bonding in

\* To whom correspondence should be addressed. E-mail: dobado@ugr.es.

<sup>†</sup> Universidad de Granada.

<sup>‡</sup> Instituto de Química Médica CSIC.

<sup>§</sup> University of Helsinki.

(1) The IUPAC defines the agostic term as those “in which a hydrogen atom is bonded to both a carbon atom and a metal atom. The term is also used to characterize the interaction between a CH bond and an unsaturated metal centre, and to describe similar bonding of a transition metal with Si-H compounds.”

(2) (a) Brookhart, M.; Green, M. L. H.; Wong, L. L. *Prog. Inorg. Chem.* **1988**, *36*, 1. (b) Brookhart, M.; Green, M. L. H. *J. Organomet. Chem.* **1983**, *250*, 395.

(3) La Placa, S. J.; Ibers, J. A. *Inorg. Chem.* **1965**, *4*, 778.

(4) Cotton, F. A.; LaCour, T.; Stanislawski, A. G. *J. Am. Chem. Soc.* **1974**, *96*, 754.

(5) Schneider, J. J. *Angew. Chem., Int. Ed. Engl.* **1996**, *35*, 1068.

(6) Fellmann, J. D.; Schrock, R. R.; Traficante, D. D. *Organometallics* **1982**, *1*, 481.

(7) (a) Brookhart, M.; Lincoln, D. M.; Bennett, M. A.; Pelling, S. J. *Am. Chem. Soc.* **1990**, *112*, 2691. (b) Burger, B. J.; Thompson, M. E.; Cotter, W. D.; Bercaw, J. E. *J. Am. Chem. Soc.* **1990**, *112*, 1566.

(8) Grubbs, R. H.; Coates, G. W. *Acc. Chem. Res.* **1996**, *29*, 85.

(9) Hirano, M.; Shibasaki, T.; Komiya, S.; Bennett, M. A. *Organometallics* **2002**, *21*, 5738.

(10) Hall, C.; Perutz, R. N. *Chem. Rev.* **1996**, *96*, 3125.

(11) Collman, J. P.; Hegedus, L. S.; Norton, J. R.; Finke, R. G. *Principles and Applications of Organotransition Metal Chemistry*; University Science Books: Mill Valley, CA, 1987.

(12) Scherer, W.; McGrady, G. S. *Angew. Chem., Int. Ed.* **2004**, *43*, 1782.

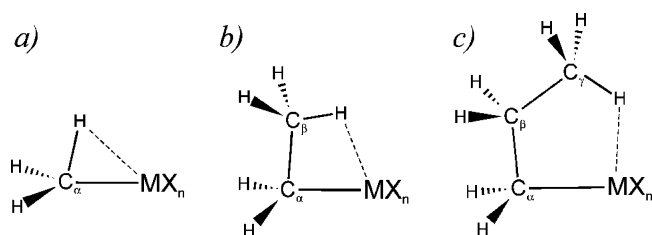


**Figure 1.** Different types of  $\text{H}\cdots\text{M}$  interactions: (a)  $\alpha$ -agostic; (b)  $\beta$ -agostic; (c)  $\gamma$ -agostic.

compounds that, in principle, show the appropriate conditions. Among others, these include a low valence electron count and an acidic character for the metal atom. A comprehensive list of these conditions can be found elsewhere.<sup>13</sup> In particular, there is still need<sup>14</sup> for theoretical studies providing a topological analysis of the electronic structure, to deepen general knowledge concerning the nature and causes of the agostic interactions.

Experimentally, agostic interactions are commonly recognized by a lower C–H stretching frequency<sup>15</sup> and a low-field  $^1\text{H}$  NMR chemical shift.<sup>16</sup> It is known that the strength of this interaction is capable even of hindering the dihedral rotation of single C–C bonds.<sup>17</sup> Depending on which carbon position links the H atom located close to the metal, the interaction is identified as  $\alpha$ -,  $\beta$ -, or  $\gamma$ -agostic bonding, and so on (see Figure 1). However, we might ask whether all of these interactions should be considered bonds.

Traditionally, the agostic bonds (or interactions) have been characterized mainly according to geometric terms, this concept being reflected in a clear deformation of the molecules where this interaction is present. In this work, we separate the geometrical and the chemical considerations relative to agostic bonding, and therefore we use the term “agostic geometries” to refer to situations where a C–H bond is placed close to a metal atom and reserve the term “agostic interactions” only for bonds or attractive interactions that justify the close metal–hydrogen distances. As will be shown below, not every agostic geometry corresponds to an agostic interaction.

Popelier and Logothetis affirm<sup>18</sup> that agostic hydrogen–metal approximations are indeed bonds and should not be misinterpreted as a special kind of hydrogen bonds, as was previously suggested.<sup>19</sup> On the other hand, three-center bonding schemes<sup>4</sup> have been proposed in addition to multiple-coordination agostic interactions,<sup>20</sup> distinguishing between “classical” arrangements with  $\eta^2$  coordination and others of recent discovery with an  $\eta^3$  arrangement. It should be mentioned that the term “agostic bonding” is being gradually replaced by the more cautious term “agostic interaction”. Even more, in the recent literature can be seen discussions about the presumed agostic nature of newly discovered  $\text{H}\cdots\text{M}$  interactions.<sup>21</sup>

Eisenstein and Jean demonstrated<sup>22</sup> that electron deficiency is not sufficient to induce an interaction with CH bonds. This

is especially relevant in those situations where a steric-free agostic geometry exists, but the conventional symptoms assigned to agostic interactions are not found.<sup>12</sup> Additionally, it is well accepted that  $\beta$ -agostic geometries prevail over the  $\alpha$  ones,<sup>23</sup> suggesting that whenever a  $\beta$ -hydrogen may exist, this is more favorable, except in the presence of steric environments.<sup>24,25</sup> Substantial differences between  $\alpha$ - and  $\beta$ -agostic geometries have already been noted in a recent review by Clot and Eisenstein,<sup>26</sup> pointing out that (a) the difficulties in predicting the existence or absence of  $\alpha$ -complexes, in contrast with  $\beta$ -complexes, (b) a direct  $\text{M}\cdots\text{C}-\text{H}$  interaction is not responsible for the distortions found in alkylidene and alkyl  $\alpha$ -agostic complexes, and (c) if present, the  $\text{M}\cdots\text{C}-\text{H}$  interaction appears to be a second-order contribution in  $\alpha$ -agostic geometries.

Different titanium complexes have been previously analyzed both experimentally and computationally, such as titanium methylidenes<sup>27</sup> and their fluorinated derivatives.<sup>28</sup> Important advances have been achieved also for Zr and Hf methylidene metal dihydride complexes.<sup>29,30</sup>

Despite the experimental and theoretical attention drawn by these kind of complexes,<sup>31</sup> even today some open issues persist, such as whether these should be considered proper bonds or how many atoms participate in the bonding. Other open topics refer to the conditions needed for the agostic distortions to appear.

From a computational perspective, the quantum theory of atoms in molecules (QTAIM)<sup>32–34</sup> and the electron localization function (ELF) analysis<sup>35</sup> are two methodologies which have been proven to reveal the nature, multiplicity, existence, or absence of bonds.<sup>36,37</sup> In a pioneering work, Popelier and Logothetis<sup>18</sup> applied the QTAIM theory to characterize several molecules with agostic geometries, concluding that these can be identified not only by the IR, NMR, and X-ray data but also purely from the electron density (experimental or calculated), indicated by the presence of an QTAIM bond path, whose properties at the bond critical point (BCP) should be about  $0.05 \text{ e a}_0^{-5}$  for the electron density and about  $0.20 \text{ e a}_0^{-5}$  for its Laplacian, while the hydrogen atom closest to the metal was characterized by an increased electron population and higher dipolar polarization. Nevertheless, their relatively restricted subject of study were only the titanium chloride alkyl complexes  $\text{RTiCl}_2^+$ , and as a result of this constricted environment around the Ti atom, their results always indicated that a clear bond path connected the H and Ti atoms. Unfortunately, this does not happen for every agostic geometry, as we show here.

In a recent comparative study on alkyl metals,<sup>38</sup> it was found that early transition metals such as Sc and Ti are able to form

(13) McGrady, G. S.; Downs, A. J. *Coord. Chem. Rev.* **2000**, *197*, 95.

(14) Pillet, S.; Wu, G.; Kulsomphob, V.; Harvey, B. G.; Ernst, R. D.; Coppens, P. *J. Am. Chem. Soc.* **2003**, *125*, 1937.

(15) Trofimenko, S. *J. Am. Chem. Soc.* **1968**, *90*, 4754.

(16) Trofimenko, S. *J. Am. Chem. Soc.* **1967**, *89*, 6288.

(17) Derome, A. E.; Green, M. L. H.; Wong, L. L. *New J. Chem.* **1989**, *13*, 747.

(18) Popelier, P. L. A.; Logothetis, G. J. *Organomet. Chem.* **1998**, *555*, 101.

(19) Bailey, N. A.; Jenkins, J. M.; Mason, R.; Shaw, B. L. *Chem. Commun.* **1965**, *11*, 237.

(20) Baratta, W.; Mealli, C.; Herdtweck, E.; Ienco, A.; Mason, S. A.; Rigo, P. *J. Am. Chem. Soc.* **2004**, *126*, 5549.

(21) Thakur, T. S.; Desiraju, G. R. *Chem. Commun.* **2006**, *5*, 552.

(22) Eisenstein, O.; Jean, Y. *J. Am. Chem. Soc.* **1985**, *107*, 1177.

(23) Jaffart, J.; Etienne, M.; Maseras, F.; McGrady, J. E.; Eisenstein, O. *J. Am. Chem. Soc.* **2001**, *123*, 6000.

(24) Guo, Z.; Swenson, D. C.; Jordan, R. F. *Organometallics* **1994**, *13*, 1424.

(25) Etienne, M. *Organometallics* **1994**, *13*, 410.

(26) Clot, E.; Eisenstein, O. *Struct. Bonding* **2004**, *113*, 1.

(27) Cho, H.-G.; Andrews, L. *J. Phys. Chem. A* **2004**, *108*, 6294.

(28) Cho, H.-G.; Andrews, L. *Inorg. Chem.* **2004**, *43*, 5253.

(29) Cho, H.-G.; Andrews, L. *J. Am. Chem. Soc.* **2004**, *126*, 10485.

(30) Cho, H.-G.; Andrews, L. *Organometallics* **2004**, *23*, 4357.

(31) Haaland, A.; Scherer, W.; Ruud, K.; McGrady, G. S.; Downs, A. J.; Swang, O. *J. Am. Chem. Soc.* **1998**, *120*, 3762.

(32) Bader, R. F. W. *Atoms in Molecules: A Quantum Theory*; Clarendon Press: Oxford, U.K., 1990.

(33) Bader, R. F. W. *Chem. Rev.* **1991**, *91*, 893.

(34) Bader, R. F. W. In *Encyclopedia of Computational Chemistry*; Schleyer, P. v. R., Ed.; Wiley: Chichester, U.K., 1998.

(35) Silvi, B.; Savin, A. *Nature* **1994**, *371*, 683.

(36) Dobado, J. A.; Martínez-García, H.; Molina, J.; Sundberg, M. R. J. *J. Am. Chem. Soc.* **2000**, *122*, 1144.

(37) Sánchez-González, A.; Martínez-García, H.; Melchor, S.; Dobado, J. A. *J. Phys. Chem. A* **2004**, *108*, 9188.

$\alpha$ -type agostic geometries easily in metal alkylidenes, but in these compounds no bond path was found. Nevertheless, the bonding scheme between metal and carbon atoms was the same for all the transition metals studied, with Ti being the element that most participates in the bond, with an elevated ionic character, which allows a broad freedom of movement to the metal atom. This makes Ti a suitable benchmark for indicating the conditions and circumstances that induce or prevent the presence of agostic-like geometries in both  $\alpha$  and  $\beta$  variants. In a previous investigation,<sup>38</sup> the causes of the close H–Ti distances in titanium alkylidenes were unknown, although the low profile of the potential energy curve on the rotation of the methyldiene unit was pointed out.

To determine fully whether the agostic geometries are caused by the Ti–C bond characteristics or whether there is a real bond participation of the alkyl hydrogen and the titanium atom, here we carry out a series of first-principles calculations on titanium complexes able to form  $\alpha$ - and  $\beta$ -agostic geometries and interactions. The principal aim of this work seeks to clarify what the differences are between  $\alpha$ - and  $\beta$ -agostic geometries, what the influence of the metal ligands is, and how the presence of agostic bonds translates into the existence of bond paths.

## Methodology

For the determination of the geometries of the molecules studied, as well as for a further analysis of the resulting electronic structures, calculations based on density functional theory (DFT) were performed with the Gaussian03 package.<sup>39</sup> Due to the good results in previous calculations on similar organometallic compounds,<sup>38</sup> we continue using Becke's three-parameter functional<sup>40</sup> with the exchange potential of Lee, Yang, and Parr,<sup>41</sup> B3LYP. Nevertheless, the most relevant data of this work have been calculated also at the MP2 level, yielding comparable data, which are provided as Table S-1 in the Supporting Information. Also, it was found that, for the best possible agreement with the experimental data, an accurate description of the electronic wave function has to be achieved through the insertion of additional polarization functions. To do so, we chose the 6-311++G(3df,2p) basis set (Pople's 6-311++G(3df,2p) basis set for C and H and the Wachters–Hay<sup>42,43</sup> basis for Ti, the latter with form (15s11p6d3fg)/[10s7p4d3fg], which contains additional 2f and g functions). The stability of all structures was checked through the eigenvalues of the Hessian matrix of second derivatives. Unless specified, the structures constitute true minima with no imaginary frequencies.

For a correct interpretation of the bonding scheme present in these compounds, it is necessary to determine whether the titanium

center and the agostic hydrogen are bonded or not. This was achieved within the QTAIM framework,<sup>32–34</sup> where the electron density topological analysis provides an accurate definition of the chemical concepts of atom, bond, and structure, as pointed out by Bader.<sup>32–34</sup> This theory allows a partition of the molecular space into separate regions associated with atoms, and thus an atom in a molecule is defined as the region of the space delimited by zero flux surfaces. From the previous definition, the concept of a bond between two atoms arises naturally. In a molecule at equilibrium, two atoms are said to be bonded if they share a common interatomic surface through which they can interact, this condition being satisfied by the existence of a zero-flux surface between them.

On the other hand, the ELF<sup>35</sup> measures the amount of electron localization, compared to an uniform electron gas, provides valuable information about the shape, location, and multiplicity of bonds, and helps in determining the causes of the agostic geometries.

QTAIM data at the bond critical points (BCPs) were calculated with MORPHY98,<sup>44–46</sup> while charges were integrated with AIM2000 software.<sup>47</sup> ELF was computed with ToPMoD,<sup>48</sup> and isosurfaces were rendered with the SciAn<sup>49</sup> visualization package. Although optimization and exploration of the PES was performed with the basis set specified above, due to the fact that most of the software used in the investigation does not support either input or output wave functions containing g functions, we performed the topological analyses from wave-functions without g functions.<sup>50</sup>

## Results and Discussion

To determine the causes that give rise to agostic geometries, we considered different molecular-model systems. These included selected titanium compounds, which were chosen as representatives of the organometallic species that may present  $\alpha$ - and  $\beta$ -agostic-like behavior, such as titanium alkylidenes and alkyltitanium species. The compounds correspond to methyltitanium **1**, titanium methyldiene **2**, ethyltitanium **3**, titanium ethenylidene **4**, and titanium ethylidene **5** (see Figure 2). The metal's substituents (X) were chosen to be either H or F atoms, in order to investigate how variations of the electronegativity of X affect the electronic equilibrium in the C–Ti bond. These variations allow altering gradually the environment around titanium, regulating the electronic pull to the metal, and will be helpful in understanding the causes of the agostic geometries.

The structures are labeled according to the following notation. The number of F atoms next to Ti is denoted with letters (a–d), and the particular conformation (eclipsed or anti) is identified with superindices and subindices.<sup>51</sup> For example, **5b<sub>F</sub><sup>a</sup>** identifies titanium ethylidene with two F atoms, where a F atom is eclipsed with respect to the C–H bond agostically close to Ti, that is taken as a reference (see Figures S-2 and S-3 in the Supporting Information for complete representations of all molecules studied and the Newman projections of those compounds with different substituents next to titanium).

Table 1 gives the main geometric parameters for the uniformly substituted derivatives of **1–5** (X = H, F). The

(38) Vidal, I.; Melchor, S.; Dobado, J. A. *J. Phys. Chem. A* **2005**, *109*, 7500.

(39) Frisch, M. J.; Trucks, G. W.; Schlegel, H. B.; Scuseria, G. E.; Robb, M. A.; Cheeseman, J. R.; Montgomery, J. A., Jr.; Vreven, T.; Kudin, K. N.; Burant, J. C.; Millam, J. M.; Iyengar, S. S.; Tomasi, J.; Barone, V.; Mennucci, B.; Cossi, M.; Scalmani, G.; Rega, N.; Petersson, G. A.; Nakatsuji, H.; Hada, M.; Ehara, M.; Toyota, K.; Fukuda, R.; Hasegawa, J.; Ishida, M.; Nakajima, T.; Honda, Y.; Kitao, O.; Nakai, H.; Klene, M.; Li, X.; Knox, J. E.; Hratchian, H. P.; Cross, J. B.; Bakken, V.; Adamo, C.; Jaramillo, J.; Gomperts, R.; Stratmann, R. E.; Yazyev, O.; Austin, A. J.; Cammi, R.; Pomelli, C.; Ochterski, J. W.; Ayala, P. Y.; Morokuma, K.; Voth, G. A.; Salvador, P.; Dannenberg, J. J.; Zakrzewski, V. G.; Dapprich, S.; Daniels, A. D.; Strain, M. C.; Farkas, O.; Malick, D. K.; Rabuck, A. D.; Raghavachari, K.; Foresman, J. B.; Ortiz, J. V.; Cui, Q.; Baboul, A. G.; Clifford, S.; Cioslowski, J.; Stefanov, B. B.; Liu, G.; Liashenko, A.; Piskorz, P.; Komaromi, I.; Martin, R. L.; Fox, D. J.; Keith, T.; Al-Laham, M. A.; Peng, C. Y.; Nanayakkara, A.; Challacombe, M.; Gill, P. M. W.; Johnson, B.; Chen, W.; Wong, M. W.; Gonzalez, C.; Pople, J. A. *Gaussian 03*, revision B.05; Gaussian, Inc.: Wallingford, CT, 2004.

(40) Becke, A. D. *J. Chem. Phys.* **1993**, *98*, 5648.

(41) Lee, C.; Yang, W.; Parr, R. G. *Phys. Rev. B* **1988**, *37*, 785.

(42) Wachters, J. H. *J. Chem. Phys.* **1970**, *52*, 1033.

(43) Hay, P. J. *J. Chem. Phys.* **1977**, *66*, 4377.

(44) MORPHY98, a program written by P. L. A. Popelier with a contribution from R. G. A. Bone; UMIST, Manchester, U.K., 1998.

(45) Popelier, P. L. A. *Comput. Phys. Commun.* **1996**, *93*, 212.

(46) Popelier, P. L. A. *Chem. Phys. Lett.* **1994**, *228*, 160.

(47) Biegler-König, F.; Schonbohm, J.; Bayles, D. *J. Comput. Chem.* **2001**, *22*, 545.

(48) Noury, S.; Krokidis, X.; Fuster, F.; Silvi, B. ToPMoD; Laboratoire de Chimie Théorique, Université Pierre et Marie Curie, Paris, 1999.

(49) Pepcke, E.; Lyons, J. SciAn 1.2; SCRI, Florida State University, Tallahassee, FL, 1996.

(50) In order to assure there is no substantial difference between the results obtained with and without the use of g functions, we compared the resulting energetic and electronic differences for **1a–5a**. These were always below  $10^{-6}$  hartree for single-point energies and electron density differences were below  $10^{-4}$  e  $a_0^{-3}$ .



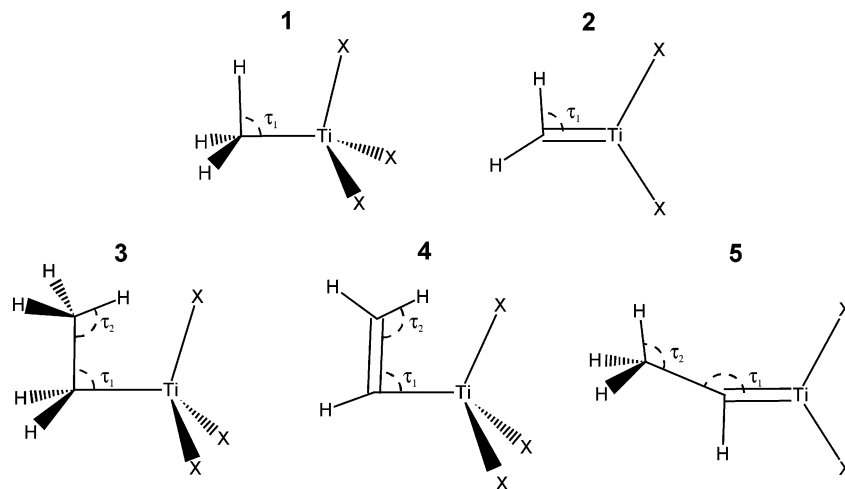


**Figure 2.** Organotitanium complexes studied: methyltitanium **1**, titanium methylidene **2**, ethyltitanium **3**, titanium ethenylidene **4**, and titanium ethylidene **5**.

**Table 1.** Selected Geometrical Parameters for **1–5** (X = H, F) Calculated at the B3LYP/6-311++G(3df,2p) Level: Valence Angles<sup>a</sup>  $\tau_1$  and  $\tau_2$  (deg) and Selected Atomic Distances (Å)

	arrangement	$\tau_1$	$\tau_2$	$C_\alpha$ -H	$C_\beta$ -H	$C_\alpha$ - $C_\beta$	$C_\alpha$ -Ti	Ti-X
<b>1a</b>	H <sub>3</sub> CTiH <sub>3</sub>	109.0		1.095			2.034	1.708
<b>1d</b>	H <sub>3</sub> CTiF <sub>3</sub>	108.9		1.092			2.052	1.767
<b>2a</b>	H <sub>2</sub> CTiH <sub>2</sub>	$\alpha$ 91.3		1.115			1.811	1.739
<b>2c</b>	H <sub>2</sub> CTiF <sub>2</sub>	123.3		1.090			1.852	1.797
<b>3a</b>	H <sub>3</sub> CCH <sub>2</sub> TiH <sub>3</sub>	$\beta$ 88.7	112.3	1.089	1.133	1.511	2.050	1.717
<b>3d</b>	H <sub>3</sub> CCH <sub>2</sub> TiF <sub>3</sub>	113.5	110.9	1.095	1.093	1.527	2.054	1.771
<b>4a</b>	H <sub>2</sub> CCHTiH <sub>3</sub>	$\beta$ 87.7	120.1	1.081	1.121	1.323	2.019	1.721
<b>4d</b>	H <sub>2</sub> CCHTiF <sub>3</sub>	121.1	122.2	1.090	1.084	1.334	2.040	1.769
<b>5a</b>	H <sub>3</sub> CCHTiH <sub>2</sub>	$\alpha$ 160.4 <sup>b</sup>	111.2	1.128	1.090	1.490	1.814	1.744
<b>5c</b>	H <sub>3</sub> CCHTiF <sub>2</sub>	137.3	112.4	1.099	1.090	1.499	1.858	1.806

<sup>a</sup> See Figure 2 for the definition of  $\tau_1$  and  $\tau_2$  angles. <sup>b</sup> For **5a**, the agostic approach occurs with the  $\alpha$ -hydrogen instead of the atom connected through the  $\tau_1$  angle, yielding a  $\angle$ Ti-C $\beta$ -H $\beta$  angle of 83.6°.

presence of agostic geometries is clearly indicated by the  $\tau_1$  valence-angle values (see definition in Figure 2), which show values close to 90° (or 160° in the case of **5a**, because of its alternative agostic geometry) when such interaction occurs. When agostic and nonagostic geometries are compared, the  $\tau_1$  angle is the only parameter that appreciably changes, the other valence angles remaining almost the same. Therefore,  $\tau_1$  will be used through this work as the key geometrical descriptor. As reflected in Table 1, agostic geometries appear only if X = H. In contrast, the presence of fluorine substituents seems to avoid these. From the common belief about  $\beta$  interactions being much more favorable than  $\alpha$  ones,<sup>23</sup> it might be expected that the agostic structure in titanium ethylidene **5a** is formed with the  $\beta$ -hydrogen, but here the stable geometry presents an  $\alpha$  geometry instead. The corresponding  $\beta$ -agostic geometry is found to be unstable, as will be shown below in the exploration of the potential energy surface (PES). The differences among structures **3a–5a** will allow a characterization of the agostic bonding, if this can be considered so.

For those alkyl chains made of two units, the angle  $\tau_2$  (valence angle  $\angle$ C $\alpha$ -C $\beta$ -H) measures the deformation of the alkyl chain

resulting from the bonding. In all cases, it presents values higher than the standard for each kind of hybridization (sp<sup>2</sup> or sp<sup>3</sup>). Minimal differences below 2° in this angle are found when comparing the values of the hydrogen-substituted vs the fluorine-substituted compounds. This indicates that the strain induced by the supposed bonds is quite reduced. On the other hand, sharper differences were found in the titanium–carbon bond distance after replacing hydrogen with fluorine next to the Ti atom. These bonds are always shortened by an amount ranging from 0.004 to 0.044 Å, independent of whether there was an agostic geometry or not. Nevertheless, the lengthening proved highest for **2** and **5**, which have in common the same C–Ti bond type.

As previously reported,<sup>18</sup> the C–H bond distances appeared to lengthen when this bond participated in the agostic arrangement, taking on values close to 1.120 Å. In contrast, C–C bonds were shortened by about 0.01 Å when any of their adjacent H atoms was close to Ti. This suggests a certain amount of C–C bond reinforcement resulting from the weakening of the C–H bond, which occurs in molecules with an agostic geometry. When **1a,d** are compared, the presence of F atoms bonded to Ti does not obviously induce shorter C–H bonds by itself. Instead, the shortening appears only when, indirectly, the F atoms cause the C–H bond to move away from the titanium atom.

All calculated conformers with homogeneous substituents at Ti presented an eclipsed conformation, except for **1d** and **3d**, which showed a staggered conformation. Because F atoms inhibit agostic geometries, it is possible to compare which geometrical parameters are also affected by the approach of the

(51) The rich variety of conformations requires also the notation of the particular arrangement of the substituents, because the presence or absence of agostic bonding is highly dependent on the positions on the substituents. For specifying this, we will use the superscripts “e” for eclipsed and “a” for anti conformations. Additionally, a subscript labels the X atom lying in the molecular symmetry plane. For eclipsed conformations, this letter indicates the nearest substituent to the C–H bond participating in the agostic bonding. For example, for **1a** there were two conformations studied (**1a<sup>e</sup>H** and **1a<sup>a</sup>H**), while for **1b** there were four (**1b<sup>e</sup>H**, **1b<sup>e</sup>F**, **1b<sup>a</sup>H**, and **1b<sup>a</sup>F**). See Figure S-3 in the Supporting Information for examples of the notation, with Newman projections.

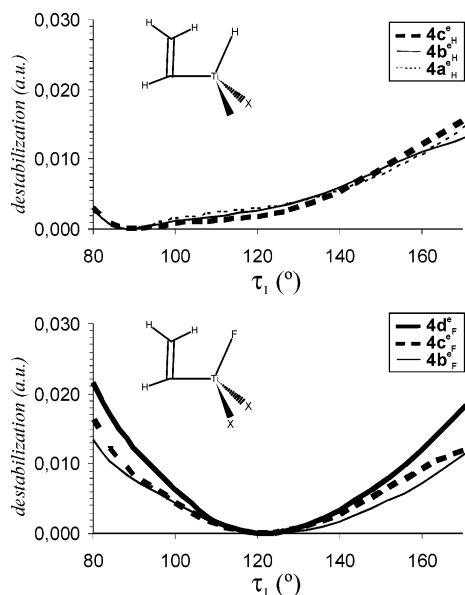


**Figure 3.** Potential energy curves corresponding to the variation of  $\tau_1$  angle for all possible combinations of X substituents of compound **4**.

H to the metal atom. In general, the C–Ti distance increases with the F substituents, as can be seen in compounds **1a,d** (about 0.02 Å). However, if this is accompanied by the destruction of the agostic geometry, this lengthening is more pronounced (about 0.04 Å). Most importantly, the C–H bond oriented toward the Ti atom is longer for molecules with an agostic geometry: about 0.02 Å for  $\alpha$ -type and 0.04 Å for  $\beta$ -type geometries. Other minor changes, such as in the length of the C–C bonds, appear to be caused only by the deviation of the standard  $sp^2$  or  $sp^3$  hybridization schemes at the  $\alpha$ -carbon.

To avoid the differences resulting from adding different substituents to the Ti atom (which could change the equilibrium in the C–Ti bond), and to distinguish the modifications induced solely by the supposed agostic interactions from those of pulling charge toward the fluorine atoms, we also studied compounds with mixed substituents at Ti, where several structures with the same number of F atoms may appear, being solely distinguished by their conformation, manifested in the element eclipsed to the closest C–H bond. It was found that, for example, for compounds with the chemical formula  $H_3CCH_2TiFH_2$ , corresponding to the two different **3b<sup>e</sup><sub>H</sub>** and **3b<sup>e</sup><sub>F</sub>** structures, the first was  $0.8 \times 10^{-3}$  au more stable than the second. Similar values were found for the other isomers: **3c<sup>e</sup><sub>H</sub>** and **3c<sup>e</sup><sub>F</sub>**,  $1.2 \times 10^{-3}$  au; **4b<sup>e</sup><sub>H</sub>** and **4b<sup>e</sup><sub>F</sub>**,  $2.3 \times 10^{-3}$  au; **4c<sup>e</sup><sub>H</sub>** and **4c<sup>e</sup><sub>F</sub>**,  $0.03 \times 10^{-3}$  au; **5b<sup>e</sup><sub>H</sub>** and **5b<sup>e</sup><sub>F</sub>**,  $5.3 \times 10^{-3}$  au. For all of these, the first conformation was more stable, presenting an agostic geometry.

Alternative geometries with  $\tau_1 > 100^\circ$  were explored for those compounds presenting an agostic geometry, but no stable one was found. In order to rule out completely the existence of these geometries, we made a detailed analysis of the PES of **3–5**. This also enabled the characterization of the energetic aspects of the agostic interactions, whenever they are found. In addition, this exploration includes the structures with mixed substituents, allowing the comparison of the relative stability of conformers differing in the nature of the substituent X closest to the agostic C–H bond.

For that purpose, the angle  $\tau_1$  was scanned from 80 to 180° in steps of 4°, optimizing the other variables at each step. Results for compound **4** are depicted in Figure 3, and those from **3** and **5** are provided as Figure S-4 in the Supporting Information.

The graphs are grouped, because of their similarity, depending on which type of substituent is eclipsed to the C–H bond.

It was found that, for all of the compounds studied, increasing the number of F atoms narrowed the main potential well around the stable conformation, but this does not necessarily imply that the agostic geometry is removed. Moreover, the number of F atoms is not related to the presence or absence of agostic geometries. In some particular cases, the presence of a single F atom is able to separate the H from the titanium, if placed adequately. This occurs whenever fluorine is placed in front of the C–H bond, suggesting that the repulsion between F and H atoms may be responsible for the removal of the agostic bonding, instead of the amount of charge around the metal center.

The PES plots showed that, for those molecules presenting  $\beta$ -agostic geometries, the curvature of the PES around  $\tau_1 \approx 90^\circ$  is more pronounced than that in other parts of the graph, there being a perceptible local distortion of the PES curve of about  $10^\circ$  width and  $\sim 2 \times 10^{-3}$  au depth. It is feasible that this feature is the energetic consequence of the presence of a true bonding interaction and that the overall PES is the result of adding two contributions: the harmonic one, resulting from the main bending of the  $\angle H-C-Ti$  valence angle, whose contribution is minimum at  $\tau_1 \approx 104^\circ$  or  $120^\circ$ , and the agostic interaction one, with a minimum at  $\tau_1 \approx 90^\circ$ . This feature is not present in the PES of the compounds presenting an  $\alpha$  geometry, such as **2a**<sup>38</sup> and **5a**, where the curve is much smoother. In particular, **2a** presents two equivalent minima, and in **5a**, the shape of the PES is very similar to that from **2a**, but with a bias that removes the minimum at  $\sim 90^\circ$  and reinforces that at  $\sim 160^\circ$ . The origin of this bias will be discussed below.

The QTAIM theory, apart from partitioning the molecular space, allows quantifying the number of bonds present in these molecules and represents a valuable tool in determining the atomic interactions. Figure 4 depicts the Laplacian of the electron density,  $\nabla^2\rho(r)$ , together with the bond paths, which identify the existence of bonds, as well as the main data for the BCPs. Complete BCP data, QTAIM charges, and Laplacian maps are provided in Tables S-5 and S-6 and Figure S-7, respectively, in the Supporting Information. From a rapid inspection of the Laplacian maps and bond paths, it can be seen that there is no systematic topological classification for the systems where the agostic geometries appear. For the  $\beta$ -type structures **3a** and **4a**, an agostic interaction can be readily identified via a bond path, linking the hydrogen atoms bonded to C and Ti, respectively, forming a five-membered HCCTiH ring, marked also with a ring critical point (RCP).

Surprisingly, the agostic interaction results in a BCP that links the alkyl hydrogen with the H bonded to Ti, in both **3a** and **4a**. We may wonder about the consequences of this particular bond path and whether this reflects an exclusive  $H\cdots H$  interaction. There are two characteristic features of this bond path: the proximity between the BCP and RCP and its highly curved shape. The first indicates a low stability of the ring topology upon perturbation of the electron density. Nevertheless, although the difference between the values of the RCP and the  $H\cdots H$  BCP is small, these are clearly distinguished in both their position and density values and its nature has been corroborated.<sup>52</sup> It is expected that the particular choice of ligands for modeling the Ti complexes may affect these results. In sharp

(52) The persistence of the  $H\cdots H$  BCP in **3a** and **4a** was verified with different methodologies (MP2 and CIS) and larger basis sets, including d functions for H atoms. In all cases, the bond path links the two hydrogen atoms.

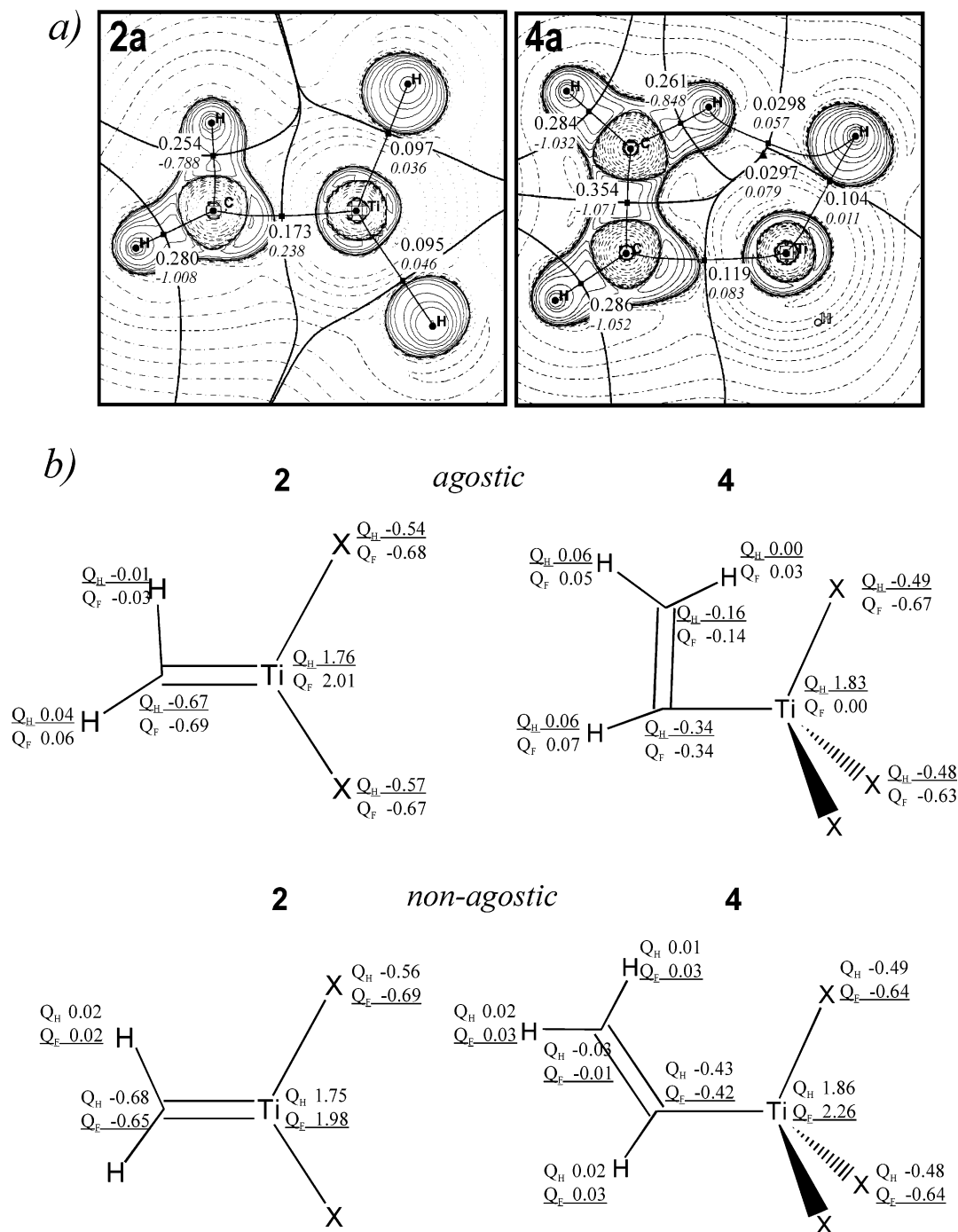


**Figure 4.** QTAIM data for **2** and **4**. (a) Laplacian plot of the electronic density for **2a** and **4a**, including the values of the electronic density  $\rho(r)$  ( $e a_0^{-3}$ ) and, in italics, its Laplacian  $\nabla^2\rho(r)$  ( $e a_0^{-5}$ ) measured at the BCP's. Bond paths are depicted with bold lines. Solid lines indicate charge-concentration zones, while dashed lines indicate charge-depletion zones. (b) QTAIM charges integrated over the atomic basins  $Q_H$  ( $X = H$ ) and  $Q_F$  ( $X = F$ ), for **2a,c** and **4a,d**, at agostic and nonagostic geometries. Depending on the compound, these correspond to the global minima or to frozen geometries, with fixed  $\tau_1$  values at 88 or 120°. Values resulting from the minimal structures are underlined.

contrast with the presence of bond paths in  $\beta$  complexes,  $\alpha$ -type geometries (with similar  $\tau_1$  angles of about 88° and the same C–H bond lengthening as the  $\beta$  complexes) show no such bond path, neither with Ti nor with any adjacent H atom. This, accompanied by the distinct PES curves, prompts consistent differences between  $\alpha$ - and  $\beta$ -agostic schemes.

Figure 4 shows the main characteristics of the BCPs found on compounds **2a** and **4a**. The remaining data for **1–5** with H and F substituents are given in Table S-5 in the Supporting Information. Regardless of whether the atomic diagram presents a bond path or not, most of the remaining QTAIM parameters were very similar for molecules with  $\alpha$ - or  $\beta$ -agostic geometry.

In all cases, the BCP of the C–H bond closest to Ti presented a lower value of the electron density,  $\rho(r)$ , its Laplacian,  $\nabla^2\rho(r)$ , and energetic density,  $E_d(r)$ , than any other BCP for the C–H bonds of the same molecule (or in the corresponding compounds with F substituents), in agreement with a lengthened bond distance and a bond weakening. The only distinct feature is the highest ellipticity,  $\epsilon$ , of the C–Ti bond in **2a**, but this is caused by the arrangement of the electron pairs around C, very similar to those present on the methylene anion  $CH_2^-$ . This occurs even for those compounds not showing agostic geometries, as in **2c**.

Other ellipticity values that merit attention are those of the  $C_\alpha$ – $C_\beta$  bonds in **3a** and **4a**, which show  $\beta$ -agostic interactions.

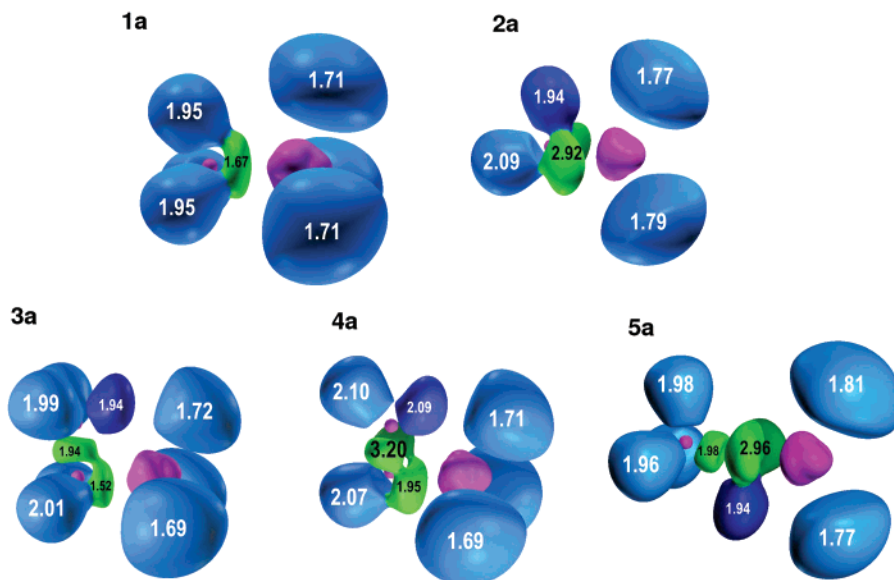


**Figure 5.** ELF isosurfaces of compounds **1a–5a** computed at a 0.7 ELF value. Numbering indicates the population of each basin. The color convention represents core basins in magenta, and the remaining valence basins are classified depending on the number of connections to core nuclear basins (synaptic order): red for monosynaptic, green for disynaptic, and cyan for disynaptic hydrogenated basins. Hydrogenated basins closest to Ti are highlighted in navy blue.

The anisotropy of these bonds is high and has a similar value, around 0.15. Nevertheless, comparing the values of those molecules with fluorine ligands, once the agostic interaction has been removed, the ellipticity recovers the nominal values for single and double bonds (ca. 0.0 and 0.3, respectively). This indicates that the agostic interaction has noticeable consequences in the neighbor bonds, and this is probably linked with the  $C_{\alpha}-C_{\beta}$  bond reinforcement observed in  $\beta$  geometries. It can be concluded that agostic interactions result not only in a weakening of the C–H bond but also in a partial restructuring of the neighboring  $C_{\alpha}-C_{\beta}$  bond. Determination of the causes of this feature is out of the scope of this article and requires further investigation.

Figure 4 also presents the population of the QTAIM atomic basins in **2a,c** and **4a,d**, in agostic and nonagostic conformations (see also Table S-6 in the Supporting Information). Depending on the compound, one of these conformations is the minimum of the PES, but the other constitutes a forced geometry with the angle  $\tau_1$  frozen at the arbitrary values of 88 and 120°, for agostic and nonagostic conformations, respectively. The charge values resulting from the stable conformation are underlined. This comparison is meant to elucidate how the charge is distributed and to show its dependence on the proximity to the titanium atom. The charge analysis indicates that, whenever a C–H bond approaches the titanium atom, the electronic population at the H atom closest to Ti is higher than that of the H not oriented toward the metal atom. This does not depend on whether or not the agostic geometry is caused by a bond (as in the case of forcing a conformation with  $\tau_1 = 88^\circ$ ). For example, in **2a**, where the minimum geometry shows a agostic-like bent geometry, the agostic H is 0.05 e more negative than the neighboring H. Nevertheless, this effect is even more pronounced for **2c** with  $\tau_1 = 88^\circ$ , in which the agostic conformation has been forced artificially. Therefore, it can be assumed that this effect is not linked to the presence of a hypothetical agostic bond with titanium but, rather, is an effect of the proximity of any metal atom. This charge distinction is normally between 0.2 and 0.6 e.

Because of these differences, the ELF was also analyzed. ELF isosurfaces for **1a–5a** are plotted in Figure 5 for a complementary discussion of the electronic arrangement in these

molecules. ELF basins and population for compounds with X = F are plotted in Figure S-8 in the Supporting Information. For those compounds presenting agostic geometries, no basin appeared between the C–H valence basin and the metal-core basin. The only visible effect is a reduction in both the volume and population of the C–H valence basin closest to the metal (basins shown in navy blue). This agrees with the previously observed BCP weakening of this C–H bond and bond lengthening. For  $\beta$  geometries, the volume reduction is greater, and an incipient deformation of the basin toward the Ti atom is noticeable, although this effect is very reduced.

Therefore, the use of the term “bond” is questionable in qualifying the  $\alpha$ -agostic geometries. To date, a clear rationalization of the causes that generate the agostic bonding has, in general, not been reported. Some hypotheses have been proposed, however, such as the assimilation to hydrogen bonding<sup>3</sup> or the statement that the attraction is of an electrostatic nature. Hydrogen bonding has been ruled out by Popelier and Logothetis,<sup>18</sup> from geometrical and electronic standpoints. However, the most accepted explanation is based on MO theory, which affirms that an interaction is caused by an overlapping of a d orbital from the metal with those from the hydrogen. This hypothesis, although plausible because metal d orbitals rule all of the behavior of transition metals, merits a rational confirmation. If it were true that overlapping of the metal’s d orbital with those of the hydrogen atoms is the cause of the bonding, this would be valid also for intermolecular bonding. From a recent review on hydrogen–metal interactions by Baratta et al.,<sup>20</sup> an exhaustive search for experimental crystallographic data in the Cambridge Structural Database for evidence of  $H\cdots M$  interactions was performed, revealing only two structures where these were present.<sup>53,54</sup>

This scarcity of experimental data prompted us to search for dimers where two simultaneous  $H\cdots Ti$  interactions were present, but all attempts to find these failed. Complementary calculations on other kinds of dimers, where a maximum number of  $H\cdots H$

(53) Evans, D. R.; Drovetskaya, T.; Bau, R.; Reed, C. A.; Boyd, P. D. *W. J. Am. Chem. Soc.* **1997**, *119*, 3633.

(54) Cotton, F. A.; Hillard, E. A.; Murillo, C. A. *J. Am. Chem. Soc.* **2002**, *124*, 5658.



contacts was present,<sup>55</sup> showed that long-range electrostatic attraction between the hydrogen atoms bonded to the titanium and those bonded to the carbon atoms was stronger if hydrogens were bonded to  $\alpha$ -carbons, the attraction with  $\beta$ -hydrogens being negligible. This is compatible with the PES curve drawn for compound **5a**. This curve notably resembles that of **2a** but is skewed. The bias and, consequently, the differentiation of the two minima is caused by a greater long-range electrostatic attraction between the titanium substituents and the alkyl hydrogen atoms. The attraction is stronger for  $\alpha$ -hydrogen atoms, thus making the  $\alpha$ -agostic geometries preferable over the  $\beta$  ones, although the same curvature is still visible. In **5a**, as in **2a**, due to the characteristics of the C–Ti bond, the symmetric double well appears; however, due to the aforementioned attraction, the  $\alpha$  arrangement is more favorable than the  $\beta$  one, but in neither case is there a bond linking these.

Given the fact that alkyl hydrogen atoms have been observed to be attracted toward the Ti center, it could have been expected that the methyl groups of **5a** have been directed toward the Ti atom, resulting in a  $\beta$  geometry with a  $\tau_1$  angle near  $90^\circ$ , this time being favored by two effects: the double minima of the alkylidene around Ti, because of the repulsion with the C lone pairs, and a possible agostic interaction. Surprisingly, this does not take place, as **5a** shows a  $\tau_1$  angle of  $160.4^\circ$ , preferring the  $\alpha$  over the  $\beta$  geometry. According to the PES, it can be seen that the plot for **5a** resembles that of **2a**, but with a contribution that polarizes the graph, destabilizing the minimum at lower  $\tau_1$  values and stabilizing that at high values, similar to a long-range electrostatic attraction or repulsion. This is another example of how the presence or absence of agostic interactions is difficult to predict. In principle, **5a** showed the same or even more characteristics as **3a** for favoring a  $\beta$ -agostic geometry, but this was not found.

Complementary to the plot of the ELF for the stable structures, a similar analysis was performed over each individual structure resulting from the PES relaxed scan for **2a**, relative to the variation of the  $\tau_1$  angle. The ELF was computed, plotted, and added together as an animation, which is given in the Supporting Information. Here, ELF pictures were taken at a value of 0.8, for a better visualization of all basins, including the cores. In this animation, it is observed how the two CH<sub>2</sub> disynaptic valence basins vary their shape, depending on the orientation angle  $\tau_1$ . In all cases, the two basins appear fused together, but for angles close to  $120^\circ$ , when these basins are placed exactly between the C and Ti atoms, the junction between those basins becomes thinner while, simultaneously, the basins are lengthened. Nevertheless, during this process the population of the basins remains almost constant (2.92 e for both). Notably, the movement of the CH<sub>2</sub> unit is accompanied by a slight change of orientation of the lobes of the Ti core basins, in such a manner that these keep pointing to the CH<sub>2</sub> valence basins instead of to the carbon core. The situation is almost identical with that for the metal alkylidene, H<sub>2</sub>CTi,<sup>38</sup> where two equivalent minima were also found, but these could not be caused by the interactions with the Ti substituents, because there are none.

From all the above, it can be affirmed that there are very low indications of the existence of a proper bonding in those  $\alpha$ -agostic-like geometries. All analyses point to a short-range repulsion between the Ti core and the alkylidene C lone pairs as the cause of the close H $\cdots$ Ti distances found in **2a** and **5a**.

Additionally, the F substituents bonded to titanium seem to disrupt  $\alpha$ -agostic geometries as well as  $\beta$ -agostic interactions. The main cause of this is found in not only the repulsion between F and H atoms but also, for **2** and **5**, the higher electronic pull from the metal to the F atoms. This, in turn, results in a lower electron population at the Ti center, thereby reducing the size of its core basins and diminishing the close-range repulsion, with a consequent flattening of the double-well potential curve.

In a search for additional confirmation, the differences between  $\alpha$  and  $\beta$  arrangements were examined. If the causes of  $\alpha$  and  $\beta$  approximations were not the same, they would react differently to an artificial elongation of the C–Ti bond. For the more flexible C–Ti bonds present in **2a** and **5a**, if a short-range repulsion were the cause of the  $\alpha$  interaction, lengthening the bond would reduce the repulsion and eliminate the H $\cdots$ Ti approach. If, on the other hand, the two alternative and equivalent agostic bonds were the cause of the two minima, then stretching the bond would not affect the existence of the agostic conformations.

For this purpose, the PES curves were plotted and displayed in Figure 6 for **2a–5a**. These are determined at fixed Ti–C bond distances, considered here as parameters. The bond distances are fixed values starting from the equilibrium C–Ti bond distances for each compound, increased in steps of 0.05 Å.

From the curves, it can be seen that, for **2a**, the double well disappears as the C–Ti distance increases, with a sensible reduction in the central maximum, indicating a reduction of the repulsion between the titanium core and the carbon lone pairs. On the other hand, for **3a** and **4a** where a bond path appears, a similar elongation does not noticeably affect the attraction to the Ti center, as the close H $\cdots$ Ti distances are preserved. Even more, the curves show how the minimum is slightly displaced to more acute angles, confirming the agostic interaction.

Nevertheless, for **5a**, the scheme is somewhat different, because of the presence of the aforementioned bias. After the C $_{\alpha}$  atom was retracted from the Ti up to 0.150 Å, the curve changes from having two concave regions and one convex region to a uniformly concave curve. Although the minimum of the curve does not turn out to be  $120^\circ$ , the  $\tau_1$  angle is reduced from  $160$  to  $155^\circ$ . The fact that the  $\beta$  geometry is not preferred even after eliminating the causes of the  $\alpha$  geometry in **5a** indicates that the precise conditions to induce  $\beta$ -agostic bonding are still unknown, because the  $\beta$  carbon (sp<sup>2</sup>) presents the same characteristics as in **4a**, the latter presenting an agostic interaction.

## Conclusions

Substantial differences between  $\alpha$ - and  $\beta$ -agostic geometries for organotitanium compounds have been found from geometrical and electronic energy standpoints, together with the QTAIM and ELF analyses. From the data calculated, it can be concluded that the term “ $\alpha$ -agostic bond” should be avoided. We recommend using the alternative expression “ $\alpha$ -agostic geometry”. Here, the term agostic is preserved because hydrogen and metal atoms are close, but, in order to eliminate a possible misunderstanding, the absence of any kind of bond linking the two atoms should be stressed.

Three main reasons underlie this conclusion: the absence of QTAIM bond paths, the characteristic potential well present on the PES for  $\beta$ - but not for  $\alpha$ -agostic geometries, and the repulsion between the carbon valence basins and the metal core shells, shown clearly by the ELF results. The differences found may apply to other transition metals, and research on this topic is under way.

(55) The geometries tested presented aligned C $_{\alpha}$ –Ti $\cdots$ C $_{\beta}$ –C $_{\alpha}$  and C $_{\alpha}$ –Ti $\cdots$ C $_{\alpha}$ –Ti bonds for each kind of interaction, in a manner that Ti substituents of the first monomer and H's of the second monomer are eclipsed with each other.



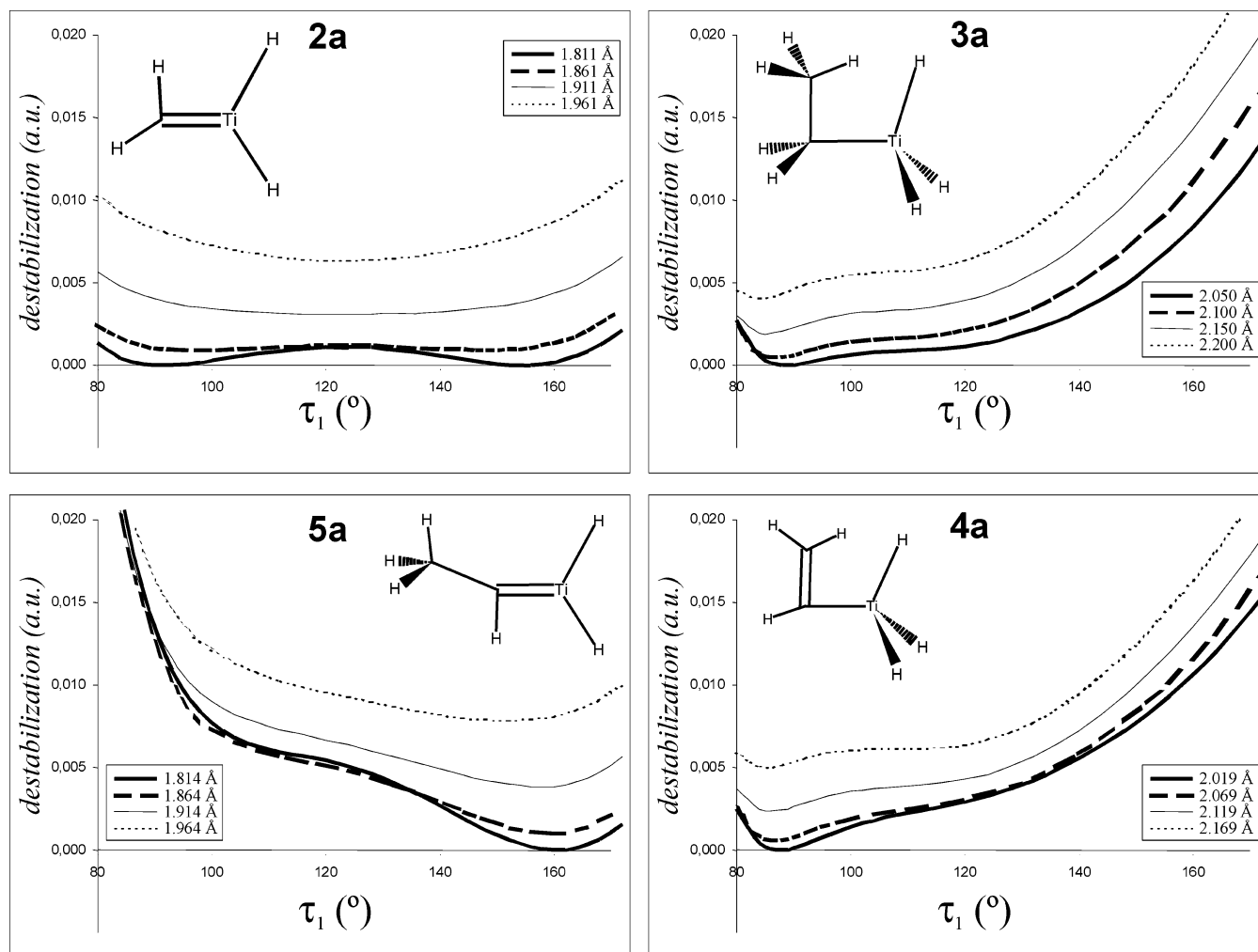


**Figure 6.** Potential-energy curves corresponding to the variation of  $\tau_1$  angle, measured at different C–Ti bond distances, in steps of 0.05 Å from the equilibrium bond distance, for **2a** and **4a**.

The  $\alpha$ -agostic geometrical arrangement occurs only for alkylidenes **2** and **5**, for which the particular distribution of the  $C_\alpha$  electron pairs conditions their whole behavior. Distinct from those alkylmetal compounds with a  $\beta$ -agostic bond, where a QTAIM bond path is measurable,  $\alpha$ -agostic geometries do not show such a bond path, indicating the absence of interaction between the H and the metal or with any of its substituents.

With regard to the PES curves resulting from varying the  $\angle\text{Ti}-C_\alpha-\text{H}$  (or  $\angle\text{Ti}-C_\alpha-C_\beta$ ) valence angle ( $\tau_1$ ), those from  $\alpha$  and  $\beta$  are remarkably different. While  $\alpha$ -agostic geometries show a mostly symmetric and smooth PES with low curvature, the  $\beta$  ones show, contained in the main bending well, a secondary narrow potential well of about  $5 \times 10^{-3}$  au depth, at values of  $\tau_1$  near  $90^\circ$ , which correspond to the shallow agostic bonding contribution. Furthermore, this feature is shown to depend on the carbon–metal distance: for  $\alpha$  geometries, after lengthening Ti– $C_\alpha$  by about 0.1 Å, the double-well curve turns into a single-well curve, while for  $\beta$ -agostic structures the described narrow potential well persists, even if the C–Ti bond length is increased by 0.2 Å. This indicates that the nature and causes of  $\alpha$  and  $\beta$  are different because, while  $\beta$ -agostic bonds maintain their characteristics, independently from the C–Ti bond, the close  $\text{H}\cdots\text{Ti}$  distances in  $\alpha$ -agostic geometries are merely a phenomenon caused by the short-distance repulsion between the metal core and the carbon valence basins, this repulsion disappearing after a minor lengthening of the C–Ti bond.

Finally, the ELF analysis of **2** and **5** together with the fact that, while varying the  $\tau_1$  angle, the C–Ti bond distance is lengthened when the  $C_\alpha$  ELF basins are placed directly between the Ti and C atom indicates a repulsion between the lone pairs from the carbon and the metal core. This repulsion is responsible for the  $\alpha$ -agostic arrangement and therefore cannot be considered to be a bond. Instead, these conformations represent a particular form to stabilize the ionic C–Ti bond with the shortest possible bond distance, causing indirectly the  $\alpha$ -hydrogen atoms to be placed close to Ti. Moreover, QTAIM results revealed that  $\beta$ -agostic interactions present a bond path, with a measurable ring critical point, while in  $\alpha$ -agostic geometries these are missing, this stressing the differences between  $\alpha$  and  $\beta$  geometries.

Overall, the effect of halide substituents next to the metal atom has two main consequences. First, the electronic pull from the Ti atom deepens the potential well for the bending of the  $\tau_1$  angle. This is caused by an increase in the positive charge at the Ti, thus reinforcing the electrostatic attraction in the C–Ti ionic bond. Second, the presence of a single F atom, placed in an eclipsed position, repels the H atom and destroys the  $\beta$ -agostic interactions and the  $\alpha$ -agostic arrangement, yielding  $\tau_1$  angles near  $104$  or  $120^\circ$ .

**Acknowledgment.** This work has been financed by the Ministerio de Ciencia y Tecnología BQU2002-01207. I.V., S.M. and J.A.D. thank the Centro y Servicios de Informática, Redes y

Comunicación (CSIRC), Universidad de Granada, for providing the computing time. Mr. David Nesbitt revised the English manuscript.

**Supporting Information Available:** Tables giving geometric and QTAIM data calculated at the MP2 level, figures giving geometrical representations of all optimized geometries, examples

of Newman projections of possible conformers, PES of **3** and **5**, complete QTAIM data and Laplacian maps for **1–5**, and ELF isosurfaces for compounds with fluorine substituents, and an animation of the ELF isosurfaces for **2a**. This material is available free of charge via the Internet at <http://pubs.acs.org>.

OM0608197